Korean Journal of Geomatics
Vol. 3, No. 1 / June 2003
pp. 43~51

Precision of Digital Photogrammetry for the Roughness Measurement of Rock Surfaces

Hyo-Sung LEE*, Ki-Won AHN, Byung-Uk PARK*** and Yong-Il KIM******

Abstract

This paper presents the benefits of using close-range digital photogrammetric techniques for measuring the roughness of rock surfaces, using digital stereo images obtained from a Rolleiflex 6006 metric camera. To precisely measure surface roughness, we researched on how to use the flat and curved reference surface obtained from geometrically corrected digital images of the rock surface by using the least squares method. To test the precision of the proposed technique, the surface roughness has been measured between the reference surface and sample areas of very smooth-surfaced rock. Then the results were compared with the measurements obtained from a laser sensor profilometer.

Keywords : *Roughness measurement, Digital photogrammetric techniques, Flat and curved reference surface, Laser sensor profilometer*

1. Introduction

Rocks used in construction or landscaping are manufactured through various methods. To assess the quality of manufactured rocks, their surface roughness is considered besides other physical factors such as gravity, absorptivity, impact strength, thermal expansion coefficient, tensile strength and friction coefficient. Good-quality manufactured rocks have a small degree of surface roughness. The roughness of rock surfaces is customarily measured using mechanical or optical equipment such as rolling bolls, light section microscopy and interferometry, speckle metrology and laser profilometry, etc. (Maerz, et. al., 1990). These methods, however, can only measure the surface roughness of small rock joints or metal segments and are unsuitable for large objects like rock masses, since this requires sampling that not only calls for much time and effort but also involves much risk as well. This is why close-range digital photogrammetry may be a more efficient method for this purpose.

To obtain a digital image in close-range digital photogrammetry, the photographed film may be scanned using a metric camera or a digital camera. With a digital camera where resolution is fixed by a CCD (Charge-Coupled Device), sensor pixel sizes of CCD arrays are not uniform and there is a lack of calibration data so precision may be low. On the other hand, a metric camera provides calibration data about lens distortion and it is possible to adjust resolution after scanning the film. Thus it has an advantage over a digital camera in closer measurement of sampling intervals of rock surface roughness.

In scanning a film photographed by a metric camera, however, various kinds of systematic errors may occur, including film deformation, lens distortion and a geometric error of the scanner (Moffitt and Mikhail, 1980). To reduce these errors, the digital

*Member, Ph. D., Research Institute of Engineering Science, Seoul National University, Korea (E-mail : hyosunglee@hanmail.net)
**Member, Professor, Dept. of Civil Eng., College of Eng., Gyeongsang National University, Researcher, Engineering Research Institute, Gyeongsang National University, Korea (E-mail : kwahn@nongae.gsnu.ac.kr)
***Member, Associate Professor, Dept. of Civil Eng., College of Eng., Hankyong National University, Korea (E-mail : ukpark@hnu.hankyong.ac.kr)
****Member, Associate Professor, Division of Urban Eng., College of Eng., Seoul National University, Seoul, Korea (E-mail : yik@snu.ac.kr)

The manuscript for this paper was received on May 27, 2003 / accepted on June 30, 2003.

photogrammetric technique is needed. This study therefore aims to correct the geometric displacements of digital images for the precise measurement of rock surface roughness through digital close-range photogrammetry using a metric camera, and to develop such method as is applicable for the reference surface (where "reference surface" implies that surface which has been mathematically determined by the least squares method with a first- and second-order equations). After that, the surface roughness of manufactured granite is compared using close-range digital photogrammetry and laser sensor profilometer. To perceive the precision of their results, the surface roughness of rock with a very smooth flat surface and curved surface is measured by the two methods

2. Methods

The 3-D coordinate system of data acquired through digital photogrammetry is different from data acquired from a laser sensor profilometer, and the roughness values of the two methods are differently represented according to the attitude conditions of the objects. For example, if a rock with a completely smooth surface is non-perpendicular to the vertical or Z-axis, its apparent roughness value appears as the slope of the object.

In this study, a method of measuring rock surface roughness using flat and curved reference surfaces is introduced (i.e., surfaces with the least differences in height in all points of the sampled area), as shown in Fig. 1, for computation of surface roughness and accurate comparison of the two methods

First, a flat reference surface is generally used in the computation of surface roughness (Swan, 1983; Kulatilake and Um, 1999; Lanaro, 2000; Fardin, et. al., 2001). It can be determined from a first-order equation, as defined in Eq. 1. The coefficients of this equation are computed using the least squares method given in Eq. 2 by the function **F**. The normal distance from the flat reference surface to an arbitrary point in the sample area is computed using Eq. 3.

$$Z = a_0 + a_1 X + a_2 Y \tag{1}$$

$$F = \sum \{Z_i - (a_0 + a_1 X_i + a_2 Y_i)\}^2 = \min. \tag{2}$$

$$di = \frac{|a_0 + a_1 X_i + a_2 Y_i - Z_i|}{\sqrt{a_1^2 + a_2^2 + 1}} \tag{3}$$

where Xi, Yi and Zi are coordinates of the arbitrary points in the sample area.

For the computation of rock surface roughness parameters when the surface of the sample area is almost curved, we have developed the curved reference surface technique. It can be applied to an external quality test or to a surface deformation analysis with the use of 3-D information on the assembly machines of the curved surface. In relation to this, EL-Hakim (1985) and Lichti, et. al. (1997) obtained the 3-D coordinates of control targets on a microwave antenna and a cylinder's surface by performing close-range photogrammetry, and analyzed surface deformation on relatively simple curved surfaces such as an elliptical paraboloid and a cylindrical surface.

The curved reference surface is determined from the second-order equation defined in Eq. 4, where the coefficients are computed using the least squares method in Eq. 5, as for the first-order equation. The normal distance from an arbitrary point Q (X_i, Y_i, Z_i) in the sample area to the corresponding point P (Xo, Yo, Zo) in the curved reference surface should be computed using a unit normal vector, as shown in Fig. 2 and Eq. 6 (Gillet, 1981; Protter and Protter, 1988; Marsden et al., 1993).

$$F = a_0 + a_1 X + a_2 Y + a_3 X^2 + a_4 XY + a_5 Y^2 - Z \tag{4}$$

$$f = \sum \{Z_i - (a_0 + a_1 X_i + a_2 Y_i + a_3 X_i^2 + a_4 X_i Y_i + a_5 Y_i^2)\}^2 = \min. \tag{5}$$

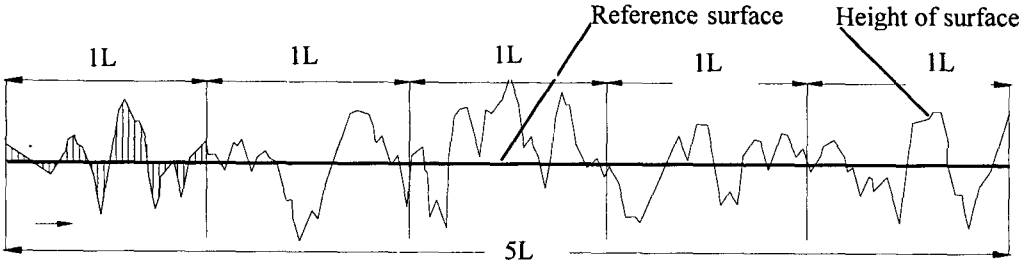

Fig. 1. Reference surface for roughness measurement.

$$n = \frac{-\frac{\partial f}{\partial X}(X0,Y0)i - \frac{\partial f}{\partial Y}(X0,Y0)j + k}{\sqrt{\left\{\frac{\partial f}{\partial X}(X0,Y0)\right\}^2 + \left\{\frac{\partial f}{\partial Y}(X0,Y0)\right\}^2 + 1}} \quad (6)$$

The equations for the computation of the position of P (*Xo*, *Yo*, *Zo*) can be obtained by reducing Eqs. 4 and 6 into Eq. 7.

$$\begin{aligned}\frac{\partial F}{\partial X}(X_0,Y_0) &= a_1 + 2a_3X_0 + a_4Y_0\\ \frac{\partial F}{\partial Y}(X_0,Y_0) &= a_2 + a_4X_0 + 2a_5Y_0\\ \frac{\partial F}{\partial Z}(X_0,Y_0) &= -1\end{aligned} \quad (7)$$

The vector between point P and Q is computed using Eq. 8.

$$\overrightarrow{PQ} = (X_0 - X_i)i + (Y_0 - Y_i)j + (Z_0 - Z_i)k \quad (8)$$

Eqs. 7 and 8 can be reduced to Eq. 9 as follows:

$$\begin{aligned}(X_0 - X_i) &= (a_1 + 2a_3X_0 + a_4Y_0)t\\ (Y_0 - Y_i) &= (a_2 + a_4X_0 + 2a_5Y_0)t\\ (Z_0 - Z_i) &= -t\end{aligned} \quad (9)$$

where t is a scale factor.

Eq. 4 can be rewritten as Eq. 10 by substituting *Xo*, *Yo* and *Zo* for *X*, *Y* and *Z*.

$$a0 + a1X_0 + a2Y_0 + a3X_0^2 + a4X_0Y_0 + a5Y_0^2 - Z_0 = 0 \quad (10)$$

P (*Xo*, *Yo*, *Zo*) is then computed from iteration using Eqs. 9 and 10. The normal distance between P and Q is calculated in Eq. 11.

$$\overline{PQ}(d_i) = \sqrt{(Xo - Xi)^2 + (Yo - Yi)^2 + (Zo - Zi)^2} \quad (11)$$

Consequently, the amplitude roughness parameters are computed using the normal distances from the curved reference surface to all points in the sample area.

The parameters representative of the roughness of a fractured surface can be grouped into various classes ranging from simple representations of amplitude, wavelength and slope to more complex statistical and frequency analysis, fractal dimension, and so on (Maerz, et. al., 1990).

In this study, we used the root mean square roughness of the height differences (d_i) of all the points on the flat or curved reference surfaces to compute the amplitude parameter of the entire surface (Eq. 12) and applied the approximate equation of Z2s (Eq. 13), this is the root mean square of the slope of the entire surface with regard to the flat reference surface, to define the properties of surface geometry (Belem, et. al., 2000).

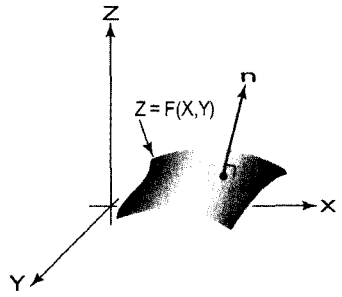

Fig. 2. Curved surface with upward unitary normal vector.

Moreover, the root mean square of the slope between the pointers (Z2) and the roughness profile index (Rp) are applied as linear parameters (Eq. 12). Z2 is a single-parameter measure that characterizes a profile based on its average slope (Myers, 1962). Rp is defined as the ratio of the true trace of the fractured surface to its projected length (L) in the fractured plane (Maerz, et. al., 1990).

$$\text{RMS} = \sqrt{\frac{\sum_{i=1}^{N} d_i^2}{N}}, \qquad Z2 = \sqrt{\frac{1}{N}\sum_{i=1}^{N-1}\left(\frac{\Delta Z_i}{\Delta X_i}\right)^2},$$

$$\text{Rp} = \frac{\sqrt{\sum_{i=1}^{N-1}(\Delta X_i^2 + \Delta Z_i^2)}}{L} \quad (12)$$

$$Z2s = \left[\frac{1}{L_X L_Y}\int_0^{L_X}\int_0^{L_Y}\left[\left(\frac{\partial Z(X,Y)}{\partial X}\right)^2 + \left(\frac{\partial Z(X,Y)}{\partial Y}\right)^2\right]_{d_X d_Y}\right]^{\frac{1}{2}} \quad (13)$$

where N is the total number of sampling points; L_X and L_Y are the nominal lengths along the X and Y axes; L_XL_Y is the area of the flat reference surface; $\triangle X$ is distance between points along sampling line; $\triangle Z$ is distance between normal points to the sampling line;

3. Test of Techniques Used

3.1 3-D Coordinates by Digital Photogrammetry

A test object used in this study is manufacturing granite (width: 75cm, height: 30cm, depth: 30cm), which is frequently used in construction or landscape purposes. Glued onto the object are asterisk-shaped targets that have 15 points from which the exterior

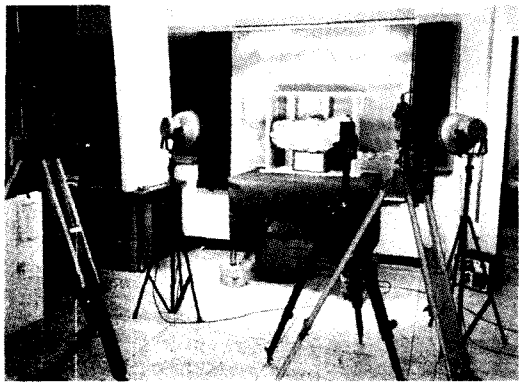

Fig. 3. View of the close-range photogrammetry set-up.

orientation of the digital image can be obtained. These targets can accomplish more precise geometric rectification in the processing of a digital image than can differently shaped targets (Ahn, 1994). Photographs are taken using the Rolleiflex 6006 metric film camera (focal length: 80.30mm) from the Rollei Fototechnic GmbH & Co. KG. It is fitted with 121 cross reseau plates described as 5mm grids to correct systematic errors (e.g., film deformation, scanning error and lens distortion). In addition, it provides calibration data for the reseau plate and lens. Fig. 3 shows equipments and test object used in the experiments.

Stereo images of the object were obtained by converging photographs of the left and right camera lenses (the base line of the camera is 1.0m, and the photographing distance is approximately 1.2m). To acquire the digital images, the film is scanned by a MICROTEK film scanner after photofinishing, with the size of each digital image being 6,000×6,000 pixels (pixel size: 0.01×0.01mm, data value: from 0 to 255). Fig. 5 shows the stereo digital images of the object acquired by metric camera.

Scanning error and film deformation are corrected into photo-coordinates of 25 cross marks. Camera principal displacement and radial lens distortion are corrected by the calibration data. Radial lens distortion, in particular, is directly corrected without control points by coefficients of the high-order polynomial offered in the calibration data and in the Newton-Raphson interpolation, which has been frequently used for the calculation of the equation's real roots. The positions of the cameras and the targets are measured by the triangulation principle using a Wild T2 theodolite (Fig. 3).

The exterior orientation parameters of the digital images acquired from the Rolleiflex 6006 camera are determined through the bundle adjustment method. The determined parameters are evaluated from the root mean square error (RMSE) of the residual errors between the positions of the check points measured by a T2 theodolite and the positions of those computed by the parameters in the digital images. Table 1 presents these results. Judging from the approximately 0.15 mm pixel size of the digital images acquired by the Rolleiflex 6006 camera, the RMSE produced relatively good results.

To generate DEM (Digital Elevation Model) of the

Table 1. RMSE of the 3-D coordinates of the check points in the digital image (unit: mm)

Coordinate	X	Y	Z
RMSE	0.104	0.097	0.210

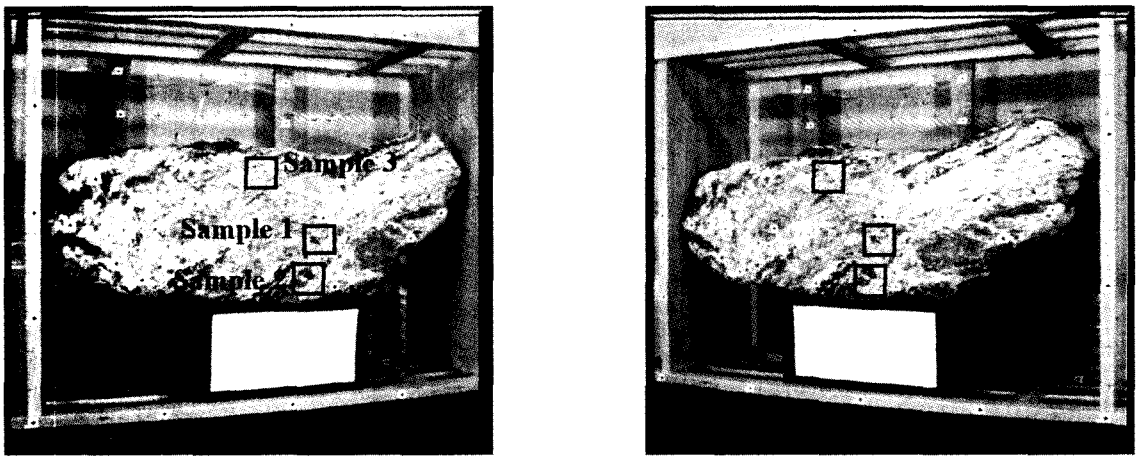

Fig. 4. Left and right images of the test object photographed by the Rolleiflex 6006 camera.

object, area-based matching method is applied by the cross-correlation function. Due to the size of the left and right digital images used in this study, processing the images takes a long time. Thus, the sample areas are trimmed in the images of the object (Fig. 4). Because significant parallax appears in the trimmed sample areas, the accuracy of matching is considerably lower. The right image therefore is matched after being geometrically corrected by adjusting to the left image that is used geometric correction tool of ERDAS IMAGINE. Matching size determined by the preliminary test is 35×35 window, and the selected search size is 65×65. Average correlation coefficients after matching of each sample areas (image sizes are all 264×264 pixel) are 0.938 to 0.953.

3-D coordinates are generated with the application of the space intersection equation using these exterior orientation parameters and conjugate points of the sub-pixel unit. This unit is calculated through the matching from the one-dimensional polynomial of the second degree.

The pixel size of all the three-dimensional positions obtained from samples No. 1, No. 2 and No. 3 is 200×200 pixels, where the real size of a pixel is about 0.15mm. Since the 3-D coordinates of each sample area that has been acquired through photogrammetry do not occur at regular intervals, we made up DEMs spaced 0.3mm apart after these had been interpolated using the inverse-weighted distance average method. Fig. 5 shows the DEMs of the sample areas, with the X, Y and Z axes having the same scale.

3.2 3-D Coordinates by a Laser Sensor Profilometer

The laser sensor profilometer used in this study is composed of a laser displacement meter, a positioning system and a computer that controls the entire profilometer system. The laser displacement meter is composed of a sensor header and a controller. The positioning system is composed of a coordinate measuring system, a servo-controller and an input part and the measurement precision of X and Y is 0.01mm. A PC computer performs data collection and processing in real time. The collected data points consist of the 3-D coordinates of the object surface formatted as ASCII and binary files.

To measure surface roughness using the profilometer, we cut sample areas spanning the approximately same area as those used in the photogrammetric technique. The heights of the sample areas were digitized with a 0.15mm spacing. The total height range was measured as 200×200 points (30×30mm). Finally, 0.3mm DEM spacing was obtained by interpolating the null value of the profilometer with the aforementioned method. Fig. 6 shows the DEMs of the sample areas obtained by the laser sensor profilometer, with the X, Y and Z-axes having the same scale.

As shown in Fig. 5 and Fig. 6, the two data sets are appeared with similar shapes, but the DEMs from photogrammetry show a smooth surface on the whole while the DEMs from the profilometry show a rough surface.

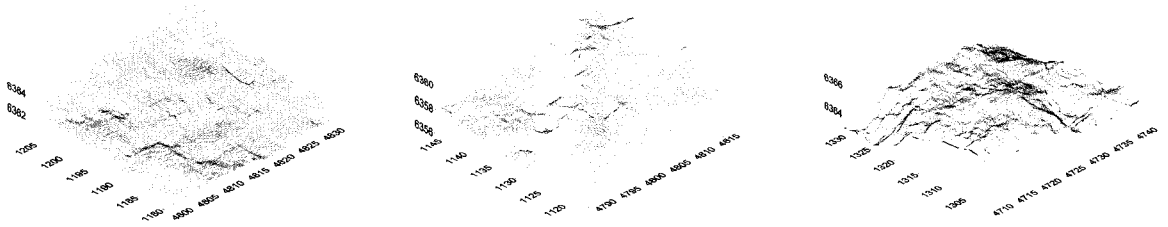

Fig. 5. DEMs of sample No. 1, No. 2 and No. 3 obtained by digital photogrammetry.

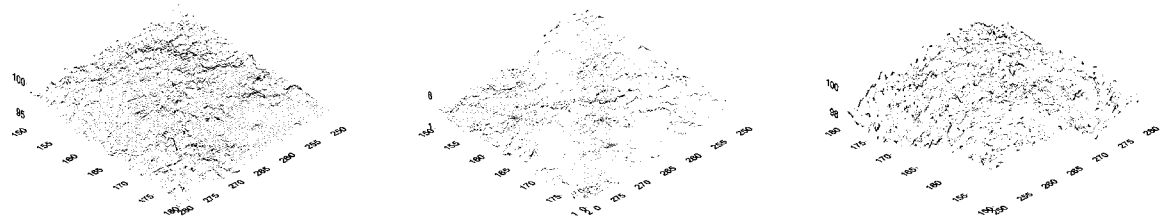

Fig. 6. DEMs of sample No. 1, No. 2 and No. 3 obtained by laser profilometry.

3.3 Measurement of Surface Roughness

Table 2 shows the RMS roughness using the normal distance from the applied reference surface to all points in the sample areas. Table 3 shows the Z2s between the flat reference surface and the sample area surfaces. Because Z2s is the parameter based on the plan, all the sample areas applied the normal distance determined from the flat reference surface. Moreover, for a quantitative comparison of surface roughness in the two methods, Z2 and Rp parameters were computed using the height of all points from the flat reference surface. Tables 4 and 5 show the Z2 and Rp means of all lines in the X and Y directions so as to compare the anisotropy of the two methods in the sample areas.

Table 2 shows that, a curved reference surface has a lower RMS roughness value (0.045 to 0.072) than a flat reference surface (0.063 to 0.085) in both methods. Table 3 shows that the Z2s values of the profilometer are 0.784 to 0.938 higher than the it's values of photogrammetry.

In the anisotropy of surface roughness of the two methods, samples No. 1 and No. 2 have similar aptitudes, but sample No. 3 produces different results (Tables 4 and 5). The reason for this is that the Z2 undulation of each line obtained by the profilometer was heavier than that obtained from photogrammetry. The Z2 parameters of all the lines obtained from photogrammetry are 0.1 to 0.4, compared to the 0.4 to 1.4 Z2 parameters of all the lines obtained by the profilometer. We take this to mean that the profilometer

Table 2. RMS roughness from the reference surface (unit : mm)

Method	Digital photogrammetry		Laser profilometer		Differences	
Reference surface / Sample area	Curved surface	Flat surface	Curved surface	Flat surface	Curved surface	Flat surface
Sample 1	0.283	0.352	0.352	0.415	0.069	0.063
Sample 2	0.277	0.291	0.349	0.376	0.072	0.085
Sample 3	0.365	0.530	0.320	0.604	0.045	0.074

Table 3. Z2s between the flat reference surface and topography

Method / Sample area	Digital photogrammetry	Laser profilometer	Differences
Sample 1	0.261	1.199	0.938
Sample 2	0.309	1.123	0.814
Sample 3	0.301	1.085	0.784

Table 4. Z2 average calculated from the flat reference surface

Method	Digital photogrammetry		Laser profilometer	
Direction / Sample area	X direction	Y direction	X direction	Y direction
Sample 1	0.145	0.162	0.721	0.886
Sample 2	0.161	0.135	0.748	0.611
Sample 3	0.237	0.176	0.686	0.795

Table 5. Rp average calculated from the flat reference surface

Method	Digital photogrammetry		Laser profilometer	
Direction / Sample area	X direction	Y direction	X direction	Y direction
Sample 1	1.012	1.013	1.191	1.263
Sample 2	1.015	1.012	1.203	1.145
Sample 3	1.021	1.016	1.175	1.224

measured height in exaggeration with random error, considering that the granite used was manufactured for construction or landscaping, as shown in Fig. 6. Results of the existing study on the measurement of the roughness parameters of artificial surfaces of granite show a Z2s parameter of approximately 0.10 to 0.30 and Rp parameters of approximately 1.010 to 1.020. Generally, the Rp of a very rough rock surface is about 1.25 (Maerz, et. al., 1995; Belem, et. al., 2000).

The resulting values of the roughness obtained by photogrammetry (where Z2s is 0.261 to 0.309 and Rp mean is 1.012 to 1.021) correspond more with that of the existing study than do the roughness values obtained by the profilometer, and appropriately represent the properties of the fractured granite surface used, as shown in Tables 3 and 5. By using the camera calibration data and suitable correction method, this result may minimize the possibility of the geometric displacement of digital images as well as the incorrect matching of stereo pairs by a significant parallax, which can be a cause for error in positions computed by digital photogrammetry. On the other hand, since the profilometer used in the test does not provide self-calibration data thereby errors in 3-D coordinate measurement may not be overcame (which can be caused by impalpable shaking and laser penetration, laser beam reflectivity and altitude of sensor header, etc.), we therefore assume that no identification and correction of these errors has been done.

4. Comparison and Assessment

To directly compare the precision of the measurement of rock surface roughness using the two methods discussed in this paper, sampling should be performed with the same intervals and ranges. In reality, 3-D information cannot be acquired at regular intervals with close-range digital photogrammetry, unlike with a laser profilometer. Resampling should thus be used to produce regular intervals in the data, in the process of which raw data may be transmuted (i.e., the original sample range can be changed).

To compare the measurement precision of the two methods, rock surfaces with very smooth flat surface and curved surface are measured, expecting that the resulting surface roughness parameters will have approximately zero value in spite of the fact that the sampling range of the laser profilometer is larger than that of photogrammetry. Fig. 7 shows left image of the rock with very smooth surface acquired by metric camera. As previously mentioned, we performed same

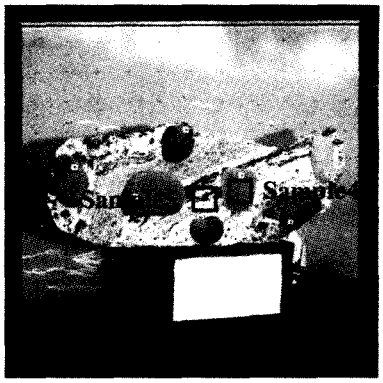

Fig. 7. Left image of appraisal object photographed by the Rolleiflex 6006 camera.

process for the acquisition of digital images, geometric rectification and 3-D coordinate determination for each method. Fig. 8 shows the DEMs of the sample areas obtained by the photogrammetry and profilometry.

To define the properties of the entire surface geometry of the sample areas, the RMS roughness and the Z2s parameter were computed between the reference surface and the sample area and compared to the precision of the two methods. Table 6 shows the RMS roughness. Sample No. 4 applied the curved reference surface, and sample No. 5 applied the flat reference surface. Table 7 shows the Z2s between the flat reference surface and the sample area surfaces.

As shown in Table 6, the RMS roughness parameters show that the profilometer computed comparatively high roughness value in sample No. 4, while photogrammetry computed high roughness value in sample No. 5. The difference between the RMS roughness values in the two methods is from 0.010mm to 0.037mm. Since the surface of sample No. 4 was smoothed in their natural state, it has higher roughness value compared with sample No. 5 whose surface was artificially cut and smoothed.

In contrast to the RMS roughness values, Table 7 shows that the Z2s value of the profilometer in sample No. 5 is higher than the Z2s value of photogrammetry. The reason for this is that roughness parameters related to amplitude largely define the wave curve in an entire surface. On the other hand, the parameters related to the slope define the delicate roughness. Thus, the correlation between the RMS roughness and Z2s is lower.

On the whole, the Z2s of the profilometer are higher (0.081 to 0.091) than the Z2s of photogrammetry. Because the sample areas used in the study were made up of very smooth planar and curved surface, photo-

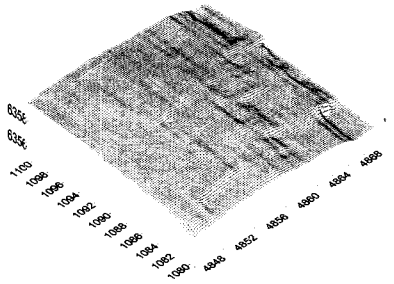

(a) Sample 4 (23×23mm) by photogrammetry

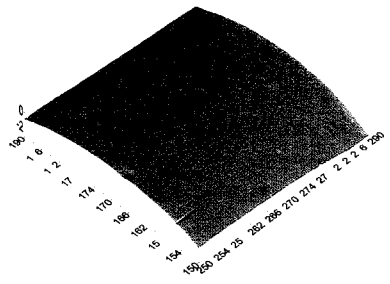

(b) Sample 4 (40×40mm) by profilometry

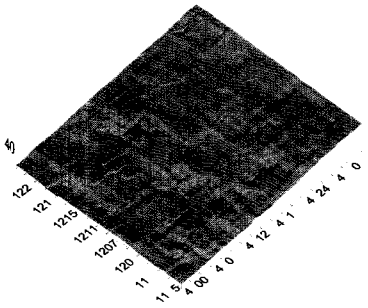

(c) Sample 5 (33×33mm) by photogrammetry

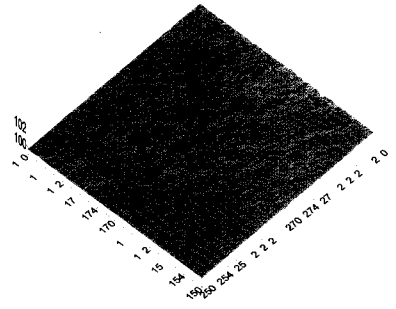

(d) Sample 5 (40×40mm) by profilometry

Fig. 8. DEM on each sample area for appraising the reference surfaces (space: 0.2mm).

Table 6. RMS roughness from the reference surface (unit : mm)

Method	Digital photogrammetry		Laser profilometer		Differences	
Reference surface / Sample area	Curved surface	Flat surface	Curved surface	Flat surface	Curved surface	Flat surface
Sample 4	0.103	-	0.113	-	0.010	-
Sample 5	-	0.078	-	0.041	-	0.037

Table 7. Z2s between the flat reference surface and sample topography

Method / Sample area	Digital photogrammetry	Laser profilometer	Differences
Sample 4	0.182	0.263	0.081
Sample 5	0.130	0.221	0.091

grammetry achieved a higher degree of precision based on the precondition that surface roughness parameters will have approximately zero value.

5. Conclusion

A close-range digital photogrammetric technique for the precision measurement of the roughness of rock surfaces is presented in this paper, using the stereo digital image obtained from a Rolleiflex 6006 metric camera. We have also developed a method that uses a curved reference surface for measuring the surface roughness of rocks related to amplitude.

In addition, the surface roughness has been measured between the reference surface and sample areas of rock with very smooth surface and compared these with measurements from a laser sensor profilometer. The resulting RMS roughness parameters were different from 0.010 to 0.037, and the resulting Z2s parameters were different from 0.081 to 0.091. Presupposing that the roughness parameters must come out near zero because the rock had a very smooth surface, the proposed method generally achieved a relatively higher level of precision in case of the rock area image is the

smooth surface. In the case of artificial fracture surfaces, the results of the proposed technique matched those of existing research.

References

1. Ahn, K. W., (1994). "Correction for scanning errors of a CCD camera scanner." Journal of the Korean Society of Geodesy, Photogrammetry and Cartography, Vol. 12, No. 2, pp. 173-180.
2. Belem, T., Homand-Etienne, F. and Souley, M. (2000). "Quantitative parameters for rock joint surface roughness." Rock Mech. Rock Eng. Vol. 33, No. 4, pp. 217-242.
3. Butler, J. B. and Lane, S. N. (1998). "Assessment of DEM quality for characterizing surface roughness using close range digital photogrammetry." The Photogrammetric Record, Vol. 16, No. 92, pp. 271-291.
4. El-Hakim, S.F. (1985). "Photogrammetric measurement of microwave antennae." Photogrammetric Engineering & Remote Sensing, Vol. 51, No. 10, pp. 1577-1581.
5. Fardin, N., Stephansson, O. and Lanru Jing. (2001). "The scale dependence of rock joint surface roughness." Int. J. Rock Mech. Min. Sci. Vol. 38, pp. 659-669.
6. Gillett, P. (1981). Calculus and analytic geometry, D.C. Heath and Company, 704-708.
7. Kulatilake, P.H.S.W., and Um, J. (1999). "Requirements for accurate quantification of self-affine roughness using the roughness-length method." Int. J. Rock Mech. Min. Sci. Vol. 36, pp. 5-18.
8. Lanaro, F. (2000). "A random field model for surface roughness and aperture of rock fractures." Int. J. Rock Mech. Min. Sci. Vol. 37, pp. 1195-1210.
9. Lichti, D. D., Chapman, M. A., Boyd, S.K., and Ronsky, J. L. (1997). "Digital photogrammetric measurement of knee joint surface." ACSM & ASPRS, Vol. 3, pp. 283-292.
10. Maerz, N. H., Franklin, J. A., and Bennett, C. P. (1990). "Joint roughness measurement using shadow profilometry." Int. J. Rock Mech. Min. Sci. & Geomech. Abstr., Vol. 27, No. 5, pp. 329-343.
11. Marsden, J. E., Tromba, A. J., and Weinstein, A. (1993). Basic multivariable calculus., Springer-Verlag, New York, pp. 50-57, pp. 398-405.
12. Moffitt, F. H. and Mikhail, E. M. (1980). Photogrammetry 3rd ed., Happer & Row, Publishers., New York, pp. 133-148, pp. 275-302, pp. 443-445.
13. Myers, M. O. (1962). "Characterization of surface roughness." Wear Vol. 5, pp. 182-189.
14. Protter, M. and Protter, P. E. (1988). Calculus with analytic geometry, Jones and Bartlett Publishers, pp. 548-551, pp. 649-651.
15. Swan, G. (1983). "Determination of stiffness and other joint properties from roughness measurements." Rock Mech. Rock Eng., Vol. 16, pp. 19-38.